Chemical Engineering Journal 478 (2023) 147428

Contents lists available at ScienceDirect

Chemical Engineering Journal

journal homepage: www.elsevier.com/locate/cej

Multidimensional cross-linked network strategies for Rapidly, Reconfigurable, refoldable shape memory polymer

Lan Luo [a], Fenghua Zhang [a,*], Linlin Wang [a], Yanju Liu [b], Jinsong Leng [a,*]

[a] Centre for Composite Materials and Structures, Harbin Institute of Technology (HIT), Harbin, 150080, People's Republic of China
[b] Department of Astronautical Science and Mechanics, Harbin Institute of Technology (HIT), Harbin, 150001, People's Republic of China

ARTICLE INFO

Keywords:
Shape memory polymer
Multidimensional cross-linked
Intrinsic thermal conductivity
Reconfigurable folds

ABSTRACT

Achieving high thermal conductivity in rigid liquid crystal-based units without compromising their super-flexibility is challenging. A strategy tacking synergistic enhancement of hydrogen bonds and liquid crystal main chains to form a multidimensional cross-linking network structure is proposed. An intrinsically thermally conductive shape memory polymers with ultra-high strength, ultra-high toughness, low-temperature resistance and wear resistance were obtained. It can lift up to 10,000 times its own weight (10 kg), has a bending radius of even 0.99 mm and remains super-flexible at −190 °C, achieving an unprecedented damage tolerance for thermosetting resins and laying the foundation for its foldability. We regulate the spherical crystal size by the solvent-induced self-assembly method, achieving an intrinsic thermal conductivity of 1.2 W/m·K. We took inspiration from the bionic structure of earwig wings combined with a crease vanishing function to apply high-aspect-ratio deployment structures in aerospace, achieving compatibility between deformation and load bearing.

1. Introduction

Shape memory polymer (SMP) has the advantages of large deformation and strong recovery capacity and may return from a temporary shape to its original shape under external excitation [1–5]. SMPs have a wide range of stiffness, programmable deformation, compound ability, massive deformation, and simple molding. SMP composites with electrical, optical, and magnetic excitation responses can be created by adding functional particles, such as carbon nanotubes and nanogold [6–11]. SMPs are actively controlled deformable materials commonly used in various fields, including biomedicine, aerospace, intelligent robotics, smart fabrics, flexible electronics, optics, and information carriers [12–21]. Thermosetting shape memory epoxy resin (SMEPs), a significant class of resins, are well known for their outstanding chemical stability and mechanical characteristics. Although the stationary phase may consist of crystalline areas, chemically cross-linked dots, or interpenetrating network structures, its primary function is to stabilize the shape of the material and force it back to its initial shape [22,23]. The key to temporary form fixation is the reversible phase, a flexible chain segment, liquid crystal phase, hydrogen bond, or coordination bond [24–26].

The unique heat-driven technique used by SMPs use cannot be pushed swiftly and responsively enough to complete the response process required in real-world situations. To suit the objectives of a spacecraft, for instance, the aerospace sector requires SMPs that can react swiftly to environmental stimuli and enable quick deployment [23,27]. To avoid breaking and cracking in the extremely low-temperature environment of space, which would shorten the life of the spacecraft, maintaining toughness is necessary. In soft robotics, SMPs offer the advantage of allowing soft robots to avoid collisions and damage by changing their shapes, thereby enhancing their safety. However, thermoset resins cannot meet these stringent requirements due to their fragility, poor toughness, and poor low-temperature resistance as dictated by their three-dimensional network structure. Unfortunately, the two properties, high strength and high toughness, are usually mutually exclusive, and it is crucial to find a solution to the conflict between toughness and strength in thermoset resins. Therefore, the sectors of aerospace, robotics, and other technologies need to provide epoxy resin with innately high heat conductivity, outstanding mechanical qualities, resilience to high- and low-temperature extremes, and wear resistance. SMPs with high thermal conductivitiy can accelerate heat transfer, increase responsiveness, and quickly complete tasks. The energy efficiency of SMPs can be enhanced by using thermal energy better.

* Corresponding authors.
E-mail addresses: fhzhang_hit@163.com (F. Zhang), lengjs@hit.edu.cn (J. Leng).

https://doi.org/10.1016/j.cej.2023.147428
Received 11 September 2023; Received in revised form 1 November 2023; Accepted 14 November 2023
Available online 17 November 2023

Although highly thermally conductive materials are frequently employed, the most direct and efficient way to increase material's thermal conductivity is to add thermally conductive particles to composites. However, this can negatively affect the material's mechanical properties. The chemical design of epoxy resins with high thermal conductivity, while retaining their shape memory performance and excellent mechanical properties, is one of the most critical issues in producing intrinsic high thermal conductivity epoxy resins. Currently, intrinsically thermally conductive thermosetting resins are primarily obtained by introducing liquid crystal units. However, a large amount of benzene ring stacking leads to a decrease in mechanical properties, and toughness is greatly sacrificed, making the strength and toughness of the material incompatible [28–31]. Structural disorder and weak intermolecular interactions are the main factors contributing to the low thermal conductivity of polymers.

Here, we propose a novel concept of constructing a multidimensional thermal conductivity network and investigate a straightforward synthetic method that can be used to adjust the heat conductivity of epoxy resins. To investigate the connection between the heat conductivity of epoxy resin and its microstructure. Fig. 1 illustrates this multidimensional crosslinking network strategy. A cross-linked network composed of covalent connections and two multilevel hydrogen bonds of various strengths can be found in the resulting shape memory epoxy resin. It can help overcome the strength-toughness tradeoff dilemma of thermosetting epoxy resins. The damage tolerance of thermosetting resins has been increased so that folds can be produced at room temperature and disappear at high temperatures, giving the resin a repeatable folding property. The creation of liquid crystal self-assembly and two-dimensional, highly ordered arrays, which promote heat transfer between polymer chains, is driven by the π-π interactions in the multidimensional cross-linked network. The polymer main chain has multiple benzene ring structures, and the molecular chain undergoes entanglement folding under the effect of π-π stacking, which improves the phonon transmission efficiency along the direction of the molecular chain. This molecular design strategy resulted in a thermosetting shape memory epoxy resin that integrates high strength and toughness, extreme cold resistance, wear resistance, and intrinsic thermal conductivity.

2. Experimental section

2.1. Materials

4,4′-Bis(2,3-epoxypropoxy) biphenyl was prepared by oneself, 4,4′-Biphenol (PPDP), hydrochloric acid, acetone, deionized water, methyl red indicator, N, N-Dimethylformamide (DMF), Ethanol, 4,4′-Diaminodiphenyl methane, 5-Amino-1H-benzotriazole, 2-Methylimidazole were purchased from Aladdin Reagent Co. Ltd.

2.2. Fabrication of SMEPs

Grafting of 4,4′-Biphenol onto the main chain of by the ring-opening reaction. The reaction was carried out in a three-neck flask by adding 4,4′-biphenol and biphenyl bisphenol glycerol ether in proportion and protected with nitrogen gas. Maintain in an oil bath at 165 °C for 30 min, then add catalyst and stir continuously for 10 h. Until the reactants in the container turn into a clear and clarified liquid. EP/PPDP-1, EP/PPDP-2, EP/PPDP-3, EP/PPDP-4, EP/PPDP5 were obtained by controlling different 4,4′-Biphenol contents including 4 wt%, 8 wt%, 12 wt%, 16 wt%, 20 wt%, respectively. The obtained epoxy monomers were tested for the epoxy values of the modified epoxy resins by the hydrochloric acid monoacetone method, and the epoxy values of SMEP-0 to SMEP-5 were 0.64, 0.59, 0.47, 0.38, 0.32 and 0.28, respectively, as shown in Supporting Information Fig. S1**(a)**.

The epoxy monomer synthesized above was kept in the container with DMF solvent because the viscosity of the high molecular weight liquid became too high. After thoroughly stirring at 120 °C, add 4,4′-Diaminodiphenyl methane reagent to the reaction at steady reflux for 20 min. The temperature is then reduced to 80 °C while stirring and adding the combined solution of 5-Amino-1H-benzotriazole-infused DMA dropwise at constant pressure. To obtain epoxy resin, the solution is poured out of the mold under 80 °C / 8 h + 120 °C / 5 h + 150 °C / 5 h for curing reaction.

2.3. Instruments

Thermal Analysis: With samples suspended in KBr particles, Nicolet-Nexus-670 Fourier Transform Infrared Spectrometer observations of the

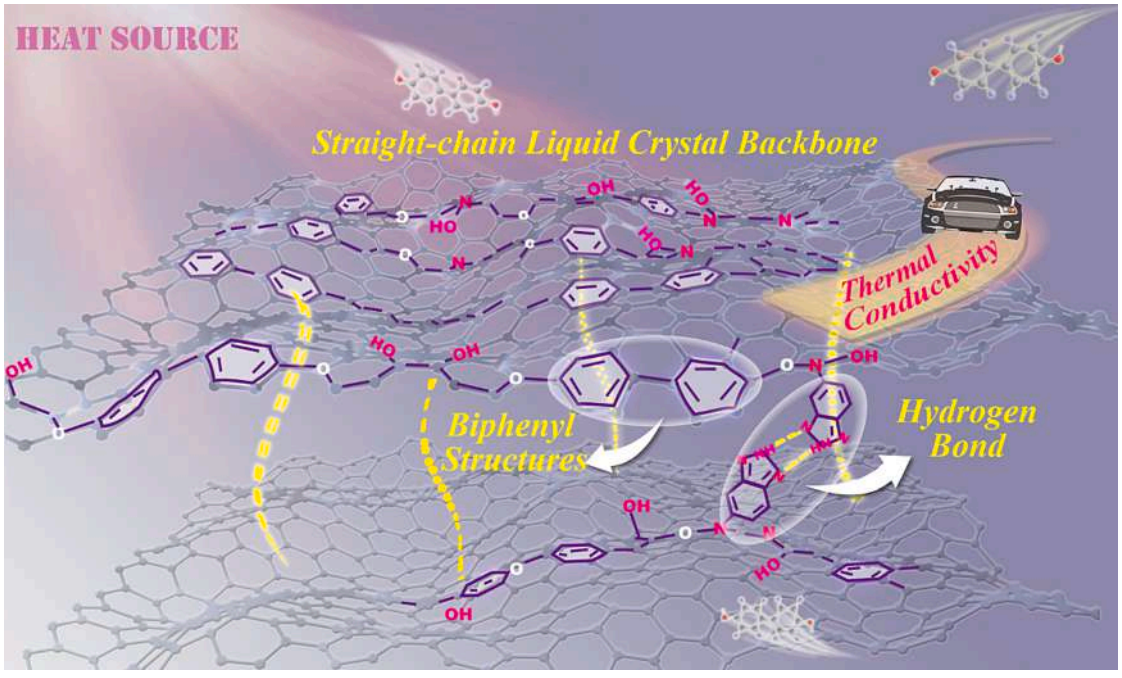

Fig. 1. Multidimensional cross-linked network strategy.

Fourier Transform Infrared Spectroscopy (FTIR) were made. To assess the molecular makeup of various epoxy curing processes, choose wavelengths between 400 cm^{-1} and 4000 cm^{-1}. Differential scanning calorimetry (DSC) was used to analyze the samples' glass transition behavior. Under a nitrogen environment, the samples were DSC scanned from 25 °C to 300 °C at a rate of 5 °C/min. The influence of the material's thermal history can be minimized by selecting a second heating cycle (all samples having the same thermal history) to detect the transition temperature. Thermal stability testing using thermogravimetric analysis (TGA). The samples were heated in a ceramic crucible with nitrogen gas at a rate of 10 °C/min from 25 °C to 800 °C. Thermal conductivity test following ASTM E 1461 standard test for thermal conductivity. The sample is 12.6 mm in diameter and 1 mm thick. The sample's top and bottom surfaces are flat and flawless, and it doesn't have any internal flaws like air bubbles or contaminants.

Tensile Tests: Tensile tests were conducted on the Zwick/Roell Universal Testing System. The samples were dumbbell-shaped, 2–3 mm thick and 8 mm wide. Tensile tests were performed at room temperature as well as at different temperatures and with a tensile speed of 2 mm/min. The mechanical behavior of constant temperature cycle at constant temperature cycle test at 50 % strain. The tensile rate was 2 mm/min to the predetermined deformation, the unloading rate was 2 mm/min, and the load was 0 N to complete a cycling experiment. The frictional wear test was performed at room temperature using the MFT-5000 instrument with a linear reciprocating motion reciprocating 10,000 times at a speed of 60 mm/s and a load setting of 30 N.

Evaluation of Shape Memory Performance: By bending, twisting, and stretching the material while applying an external force, the shape memory behavior was evaluated. They were quickly molded and quickly chilled to solidify after being heated to Tg and becoming soft. This gave them a transitory shape.

3. Results and discussion

3.1. Properties of the SMEPs

The SMEP synthesis procedure is depicted in Fig. 2**.** After a period of reaction, the mixture of PPDP and biphenyl bisphenol glycerol ether changed from an opaque and turbid liquid that it was before the addition of the reaction catalyst to a homogenous and transparent liquid. The appearance of a clear liquid indicates a chemical reaction, which is due to an addition reaction between the epoxy group and the hydroxyl group, resulting in the introduction of more benzene ring groups into the main chain. Additionally, when the PPDP content rises, the color of the resulting epoxy monomer with inherent heat conductivity rapidly deepens, as seen in the figure. Furthermore, we opted for 4,4′-diaminodiphenyl methane with a symmetrical structure to carry out the crosslinking reaction. The introduction of hydrogen bonds into the cross-linked network is made possible by the addition of 5-amino-1H-benzotriazole, which contains a hydrogen bond donor and acceptor. This results in the formation of a covalent bond and a cross-linked network with two distinct strengths of multi-level hydrogen bonds. Using a simple and controllable one-pot synthesis approach, the thermal conductivity of the synthesized epoxy resin is changed by altering different raw materials or raw material ratios to build a multi-dimensional thermal conductivity network.

Fig. 3**a** depicts a schematic of the network structure of the intrinsically thermally conductive epoxy resin. Due to the large number of benzene rings arranged in the polymer backbone, the deflection angle of the whole molecular chain segments is reduced, presenting a straight-chain type of liquid crystal backbone. The structure of the molecular chain segments is almost overlapped when viewed from the side, which proves the degree of neatness of the molecular chain segments. Fig. S1**b** illustrates the infrared spectral profiles with the addition of different contents of PPDP epoxy monomers, and Fig. 3**b** shows the locally magnified FTIR spectra. The modified epoxy exhibited a strong absorption peak at approximately 3500 cm^{-1}. The intensity of the absorption peak increased in proportion to the amount of PPDP, which can be attributed to the stretching peak of the –OH group of the epoxy resin following its modification by PPDP. Furthermore, it can be deduced that the introduction of PPDP creates more –OH groups, as shown in the reaction process in Fig. 2. The DSC curve of the SMEP system is shown in Fig. 3**c**, and the shift in the curve typically reflects the glass transition temperature (Tg) of the thermosetting resin. The steep peak of the curve indicates that Tg increased steadily as the PPDP content increased. This might be attributed to the addition of the biphenyl structure, which increases the intermolecular contact forces and degree of molecular cross-linking, improves the hardness and stability of the substance, and increases Tg. The GPC leaching curves of various epoxy monomers are shown in Fig. 3**d** as the content of PPDP gradually increased. The GPC

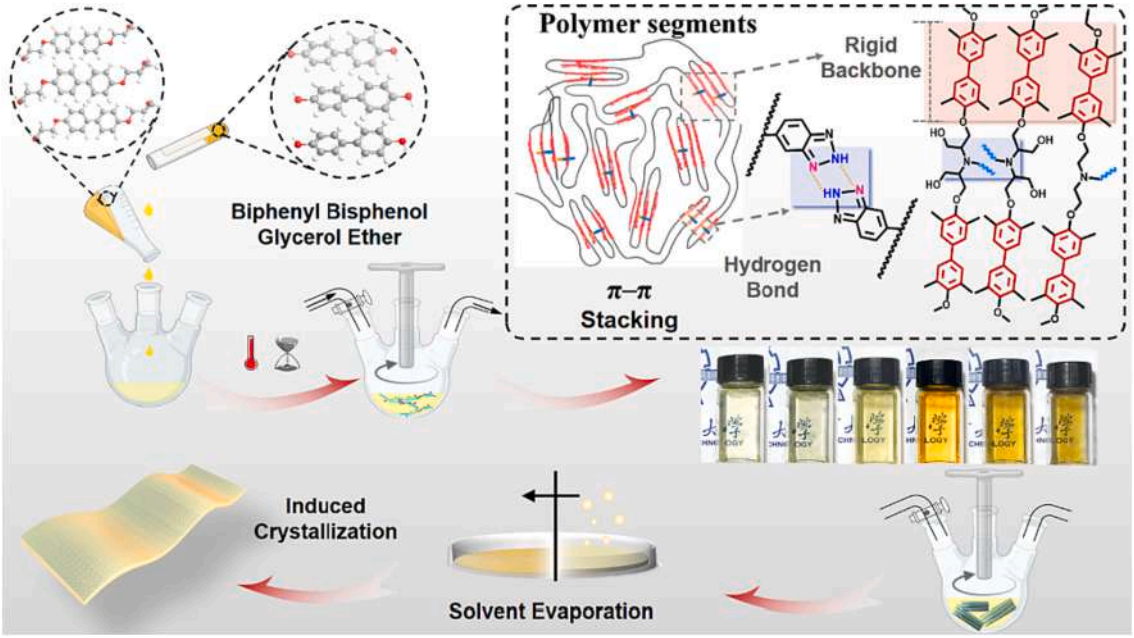

Fig. 2. Schematic diagram of the synthesis process of SMEPs system.

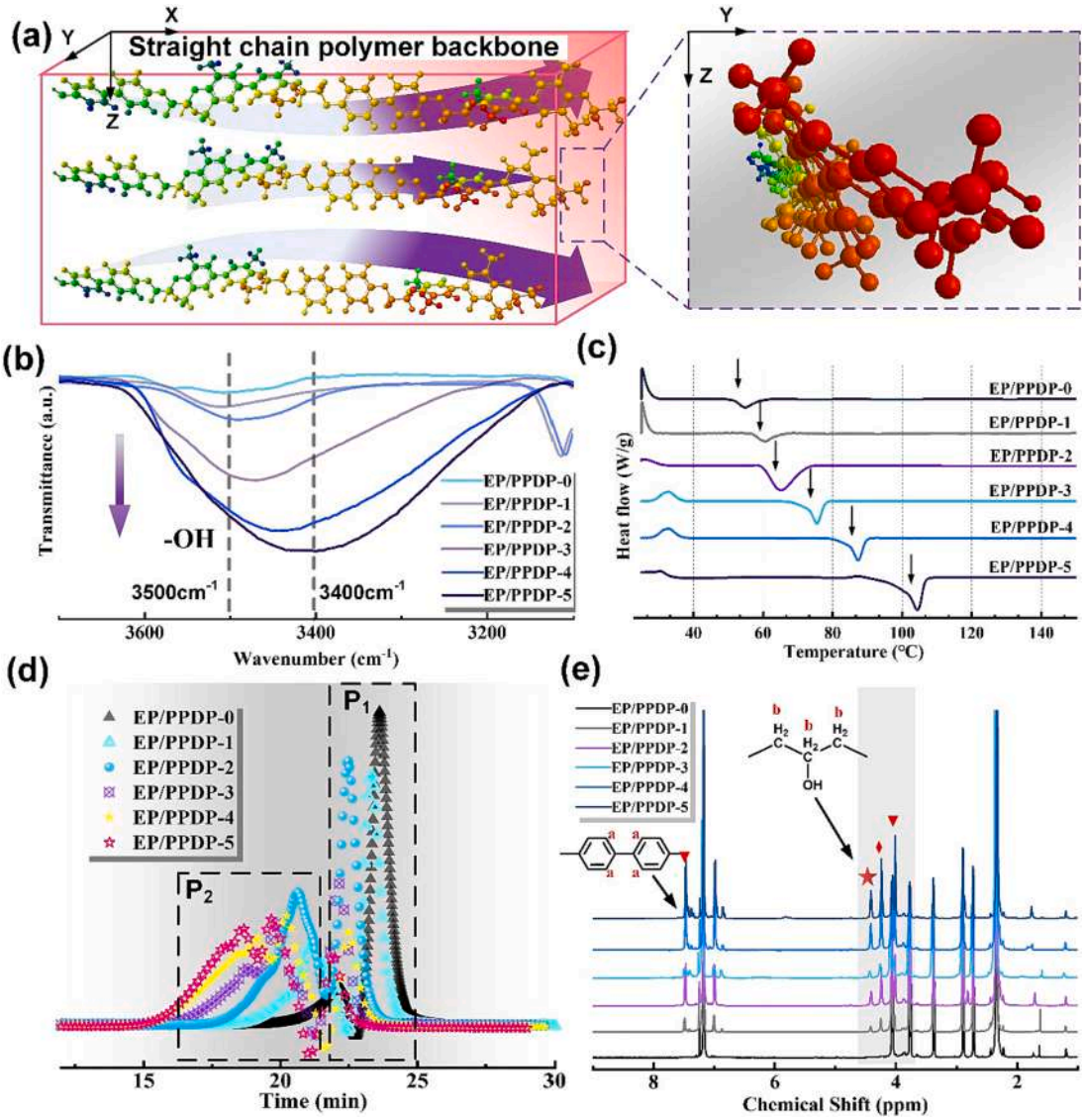

Fig. 3. **(a)** Schematic diagram of the main chain structure of a straight-chain liquid crystal. **(b)** FTIR curves of epoxy monomers. **(c)** DSC curves of epoxy monomers. **(d)** GPC efflux curves of epoxy monomers. **(e)** ^{1}H NMR curves of epoxy monomers.

leaching curves of each epoxide monomer had two peaks P_1 and P_2. Under the action of a catalyst, an addition reaction occurs between the epoxy group and the hydroxyl group, leading to etherification and the formation of new hydroxyl groups.The GPC efflux curve revealed that the peak area of various epoxy monomers increased with increasing PPDP addition, whereas the peak area of small molecular weights decreased with increasing 4,4′-biphenol addition, indicating that PPDP was successfully introduced. Fig. 3**e** presents the ^{1}H NMR spectrum of the PPDP-modified epoxy resin. The incorporation of PPDP led to the emergence of a novel absorption peak at approximately 7.5 ppm, which was ascribed to the proton hydrogen of the biphenyl structure of PPDP. Additionally, the absorption peak at around 4.3 to 4.4 ppm corresponded to the proton hydrogen on the added hydroxyl group, and the peak also exhibited a broadening effect.

Fig. 4**a** shows the DSC test results for all samples. With the increase in the content of introduced PPDP, the Tg in the DSC curve steadily increased, which may be due to the increase in the benzene ring content in the introduced monomers, thereby increasing the Tg of the polymers. The FTIR curves of the intrinsically thermally conductive SMEP system are shown in Fig. 4**b**, with progressively higher peaks from 3570 cm^{-1} to 3450 cm^{-1}. This indicates that more –OH groups were added to the monomer after the addition of various PPDPs, forming stronger intramolecular hydrogen bonds. Simultaneously, no epoxy group peak was observed at 910 cm^{-1}, showing that the epoxy group was involved in the ring-opening reaction. A peak attributable to N-H was observed at 1200 cm^{-1} to 1350 cm^{-1}, which was brought about by the insertion of the –NH bond in 5-amino benzotriazole. Fig. 4**c and d** display the thermal weight loss curves and local amplification curves of SMEP after the addition of 4,4′-biphenol to the backbone. TGA measurements were performed to examine the thermal stability of the intrinsically thermally conductive SMEP cures. The weight-loss temperature and final residual carbon rate at 5 % were derived from the graph. The introduction of PPDP played a crucial role in improving the thermal stability of intrinsically thermally conductive SMEP resins. With the increase in the amount of PPDP, the heat loss curve gradually shifted to the high-temperature region and the decomposition temperature and residual carbon rate increased significantly. For instance, the decomposition temperature and the final residual carbon rate at 800 °C were raised to 365 °C and 28 %, respectively, when the PPDP content was 25 wt%. Additionally, hydrogen bond formation can increase the crosslinking density of molecules, thereby improving the mechanical and thermal properties of materials.

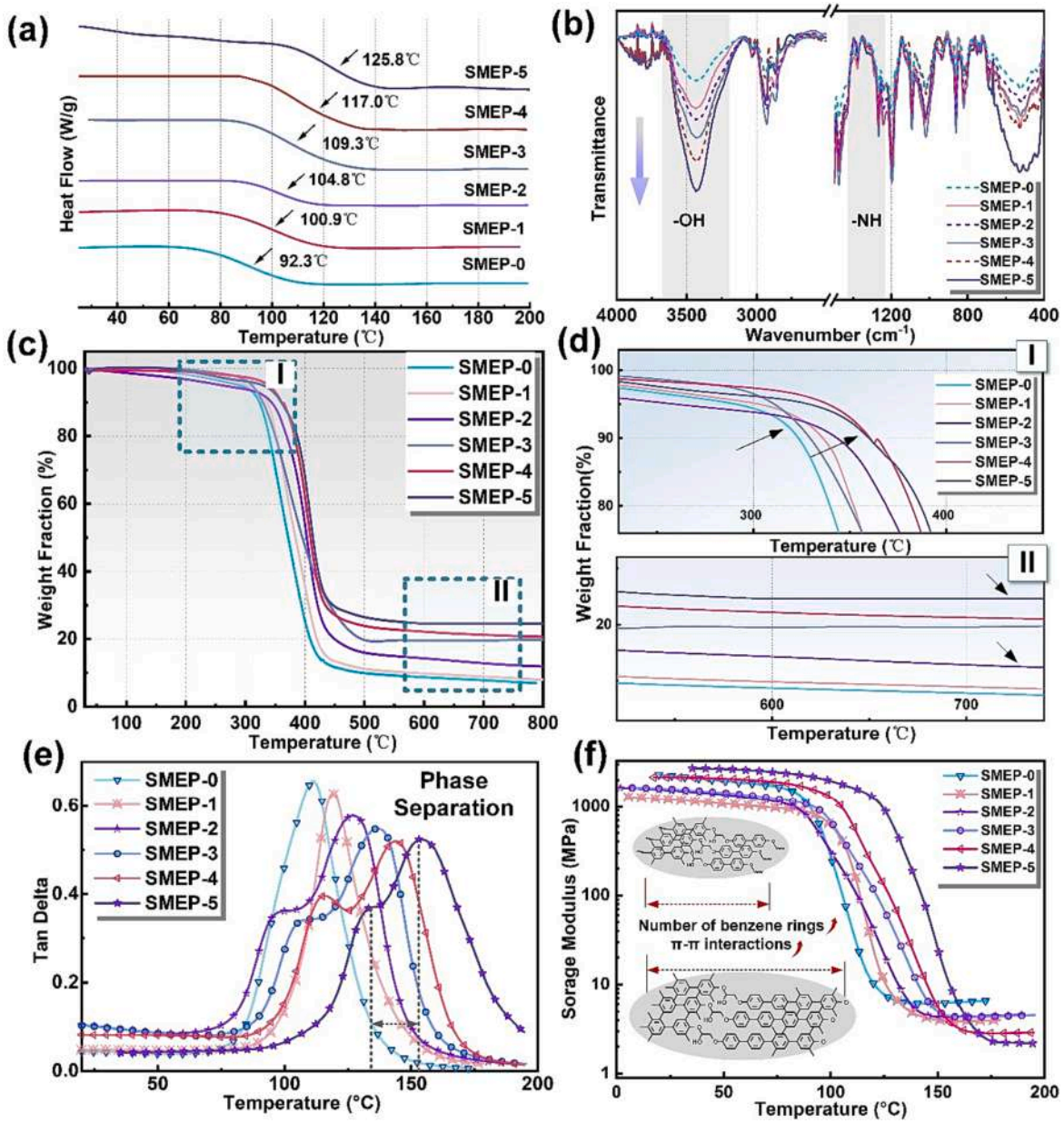

Fig. 4. **(a)** DSC curves of SMEPs system. **(b)** FTIR curves of SMEPs system. **(c)** TGA curves of SMEPs system. **(d)** SMEPs system local amplification TGA curves. **(e, f)** DMA curves of SMEPs system.

The results of DMA testing of the SMEP system are shown in Fig. 4**e**, which demonstrates how one peak gradually split into two different peaks with the increase in the amount of PPDP. This might be attributed to the crystallization behavior induced by the biphenyl structure, which causes the matrix to crystallize in various shapes, including both crystalline and amorphous regions. The Tg is an important parameter for evaluating thermosetting shape memory resins. The DMA curve of SMEP-0 only displayed a single peak Tg of 106 °C, whereas Tan δ progressively displayed two Tg peaks with the increase in the amount of PPDP added. Fig. 4**e** unequivocally indicates that the addition of PPDP significantly increased the Tg of the intrinsic thermally cured epoxy. For instance, the Tg of SMEP-5 is elevated to approximately 154 °C. This might be because PPDP was introduced at a uniform growth rate in all directions, gradually forming a micron-sized spherical crystal structure. Phase separation occurred when more spherical crystals were formed as the number of benzene rings increased with the addition of PPDP. Following the trend of the Tg, the energy storage modulus of the SMEP increased with increasing PPDP content (Fig. 4**f**). The incorporation of PPDP enhanced the heat resistance and mechanical properties of the resin.

3.2. *Thermal performance*

Through conjugation between the aromatic groups, the molecular chain has a relatively linear structure. There is a conjugated π electron system between the benzene rings in the biphenyl ring, and this conjugation can shorten the bond length between the benzene rings, resulting in a relatively linear structure of the molecular chain (Fig. 5**a**). Additionally, hydrogen-bonding interactions exist between the main chains, which can make the molecular chains compact and linear. All the physical images of the SMEP samples are visually compared in Fig. 5**b,** which shows that the color of the samples deepened with the increase in the PPDP content. Owing to the increase in crystallinity and the expansion of the crystal size, SMEP-5 appeared almost opaque. Because an ordered structure creates a channel that facilitates phonon transfer, polymers with ordered structures typically exhibit better thermal

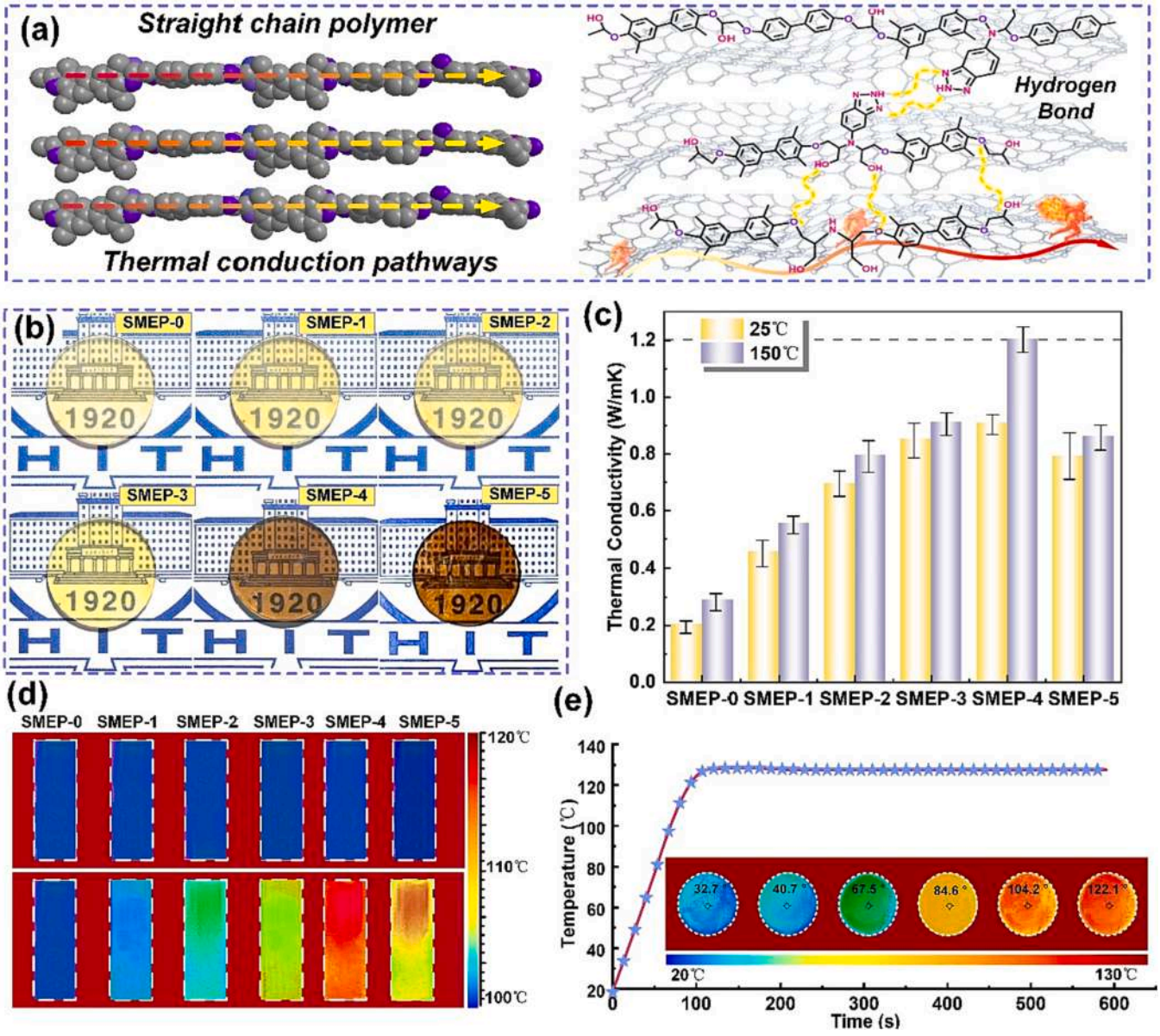

Fig. 5. **(a)** Intrinsically thermally conductive molecular design schematic. **(b)** Physical view of SMEPs sample. **(c)** Thermal conductivity of SMEPs at different temperatures. **(d)** Thermal conductivity of SMEPs samples simultaneously under a heating table set to 120 °C. **(e)** SMEP-4 sample heat transfer under a heating table at 130 °C.

conductivities. Hence, the intrinsically thermally conductive epoxy cures with a spherical crystal structure have higher thermal conductivity than those with regular epoxy cures. Test results indicated that adding PPDP resulted in high heat conductivity in the SMEP cures. As shown in Fig. 5**c**, the thermal conductivities of the samples, SMEP-1 to SMEP-4 gradually improved after the addition of increased levels of PPDP compared to SMEP-0, whereas the thermal conductivity of SMEP-5 decreased. This is due to excessive PPDP content, which leads to more benzene rings on the main chain and more π - π stacking non covalent bonding, which is beneficial for the growth of spherical crystals. Moreover, larger spherical crystal size leads to an increase in intermolecular distance, thereby reducing intermolecular interactions and decreasing thermal conductivity. SMEP-4 has a thermal conductivity of approximately four times higher than regular epoxy resin. As previously indicated, a key element in increasing thermal conductivity is the ordered spherical crystal structure of the epoxy resin, which is innately thermally conductive. The crystallinity of polymer spherulites can affect their thermal conductivity. Typically, polymers with high crystallinity have high thermal conductivity. This is because the molecular arrangement inside the crystal is more orderly, and heat can be effectively transferred through close contact between molecules. An increase in grain size may lead to a decrease in the number of grain boundaries, weakening obstacles to thermal conductivity, and thus improving thermal conductivity. However, excessive grain size may lead to an increase in isolated molecular regions within grain boundaries, thereby reducing thermal conductivity. The capacity to transport heat in the direction of the epoxy resin backbone was enhanced by the addition of a stiff PPDP biphenyl structure. Simultaneously, thermal conductivity is higher at high temperatures than that at room temperature because, at high temperatures, the thermal motion of polymer molecules is intense, the interaction forces between molecules weaken, and heat conduction becomes easy. We compared our work with the reported intrinsic thermal conductive resin in terms of thermal properties[32–37]. The comparison results are shown in **Table S1**. As shown in Fig. 5**d**, the SMEP samples were placed simultaneously on a heating table at 120 °C to track the variability of heat transfer for samples with various thermal

conductivities. SMEP-4 reached 120 °C rapidly, as can be observed visually. The surface temperature of the 1.5-mm-thick disc reached 122.1 °C within 100 s, as shown in Fig. 5**e**, which tracks and records the heat transfer of the SMEP-4 sample under a heat source of 130 °C.

3.3. Mechanical performance

Fig. 6**a** shows a schematic of the molecular design of SMEP. The spherical crystal structure of polymers can increase their strength because it is highly ordered and compact, further enhancing the strength and rigidity of the polymer. The tensile stress–strain curves of the SMEP system are shown in Fig. 6**b**, and both the strength and strain increased with increasing PPDP content. SMEP-4 achieved the highest tensile strength of 101 MPa, whereas SMEP-5 exhibited the highest strain of 23 %. Because of the interlocking of hydrogen bonds in the crosslinked network, excessive movement or sliding of polymer molecules under stress can be prevented, which can increase the tensile strength and toughness of the polymer. Both the strength and modulus exhibited an increasing trend, followed by a decreasing trend with increasing PPDP content. This might be because an increase in crystal size leads to an increase in the irregularity of the crystal structure, resulting in a decrease in the crystallinity of the polymer and a looser arrangement of molecular chains, which leads to a decrease in the mechanical properties of the polymer. SMEP-4, with a thickness of 0.3 mm, can support a weight 10,000 times its weight, equivalent to a weight of 10 kg, with a lever arm of 2 cm. The ordered arrangement and tight structure of the π-π stacking between the benzene rings leads to the creation of spherical crystals of different sizes. The regular arrangement of the benzene rings and the hydrogen bonding structure is effective in transferring externally applied forces throughout the polymer (see Movie S1). SMEP can be bent at room temperature to a limiting value of less than 1 mm bending radius. At a certain hydrogen bond density in polymers, the distance between molecular chains is relatively large, and the movement of molecular chains is relatively free. This flexibility can make the material more prone to deformation and plastic deformation. It demonstrates an unprecedented compatibility effect of ultra-strength and ultra-toughness of epoxy resin. (Fig. 6**c**). The hydrogen bonding between multidimensional networks can increase the cross-linking and bonding

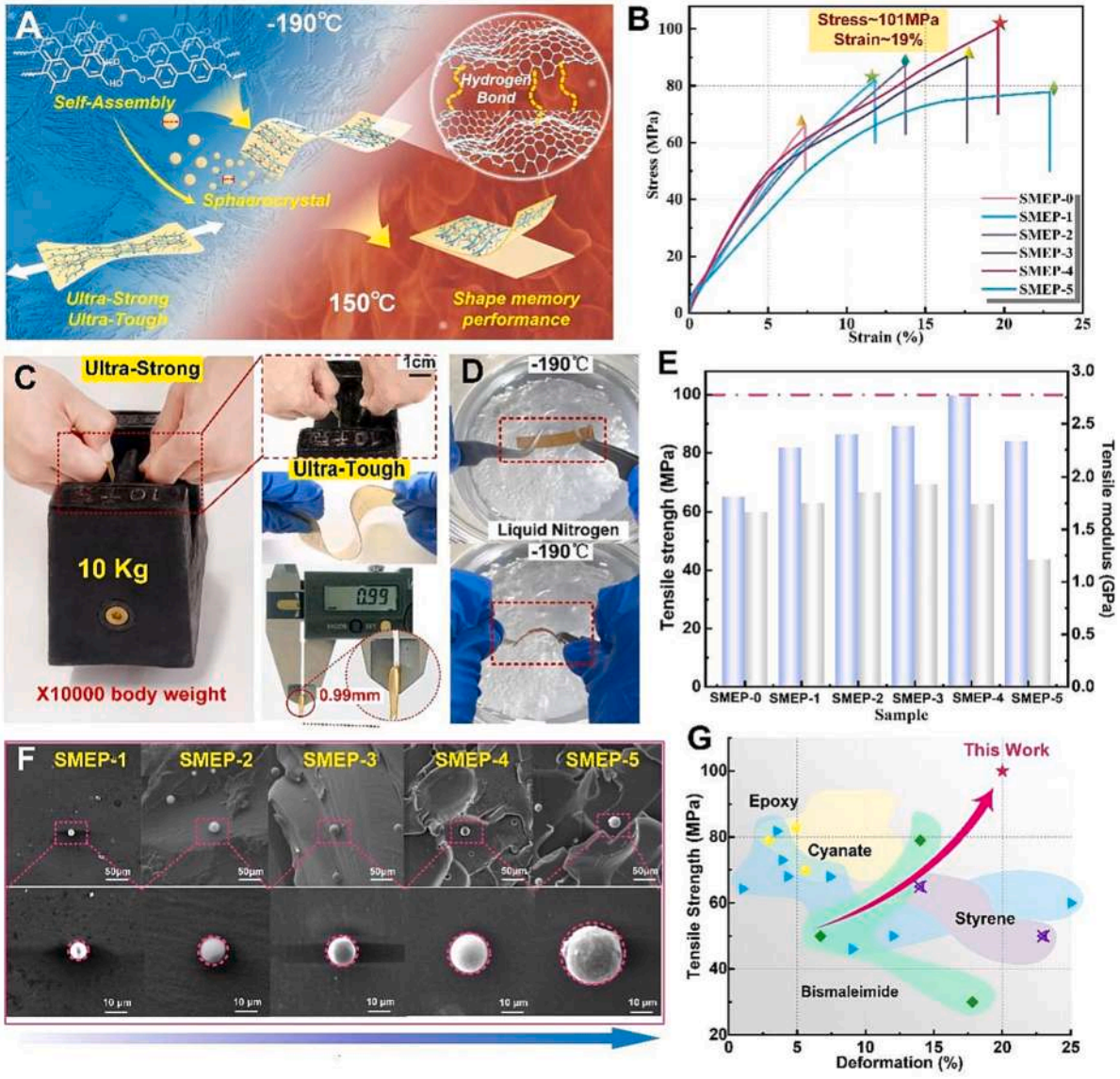

Fig. 6. **(a)** SMEPs with outstanding mechanical properties are shown schematically in the diagram. **(b)** Tensile strain–stress curves of SMEPs at room temperature. **(c)** SMEPs can withstand the weight of 10 kg weights and folding limit curvature radius reaches 0.99 mm at room temperature. **(d)** SMEPs maintain their flexibility in liquid nitrogen. **(e)** Comprehensive mechanical properties of SMEPs. **(f)** SEM images of SMEPs cross-sections. **(g)** Comparison chart of SMEPs and thermosetting resins.

strength between molecular chains, thereby making materials more stable and resilient. High density hydrogen bonds can enhance the interaction between molecular chains, making materials more wear-resistant and heat-resistant, able to resist external pressure and deformation, and to some extent, prevent brittle fracture of materials. These mechanical properties were also discovered for the first time in epoxy resins. Additionally, the SMEP films can be easily folded and bent at room temperature (Fig. 6**d**). Due to the presence of hydrogen bonds, thermosetting epoxy resin has unprecedented flexibility in extremely cold environments (-190 ℃). Epoxy resin still maintains excellent flexibility under liquid nitrogen and can be bent arbitrarily (Movie S2).

Fig. 6**e** shows the tensile strength and modulus of the SMEP system. Thus, the damage tolerance of the material is greatly improved, laying the foundation for the subsequent origami work, so that the material can be bent until it leaves a crease. Biphenyl-structured polymer molecules can bind together in solution to form aggregates. Owing to their stiffness, polymer molecules with biphenyl structures have the propensity to aggregate into planar forms. These planar structures pile up on top of one another to build spherical structures, eventually forming spherulites as the polymer molecules continue to aggregate. Biphenyl-structured polymer spherulites exhibited high degrees of stiffness and organization. When the content of PPDP increases to 20 wt%, the spherulite size gradually increases, interaction between polymer chains decreases, and molecular chains can move and deform more freely, thus improving the toughness of SMEP-5. When the size of the spherulites is large, the interchain force is weak, and the strength of SMEP-5 decreases. The size of the spherulites increased with the increase in the molecular weight of the polymer because strong intermolecular interactions increased the molecular weight of the polymer. The size of the spherulites increased with the increase in the concentration of PPDP (Fig. 6**f**). As shown in the DMA curve of Fig. 4**e**, it gradually splits into two distinct Tg peaks with increasing PPDP content. We compared the mechanical properties of SMEP prepared in this study with those of other thermosetting resins and found that SMEP has both strength and toughness at room temperature, surpassing other thermosetting resins reported to date [5,38–44]. Therefore, this research paves the way for producing SMPs with improved damage tolerance that can be used in various fields, which require unprecedented mechanical properties (Fig. 6**g**).

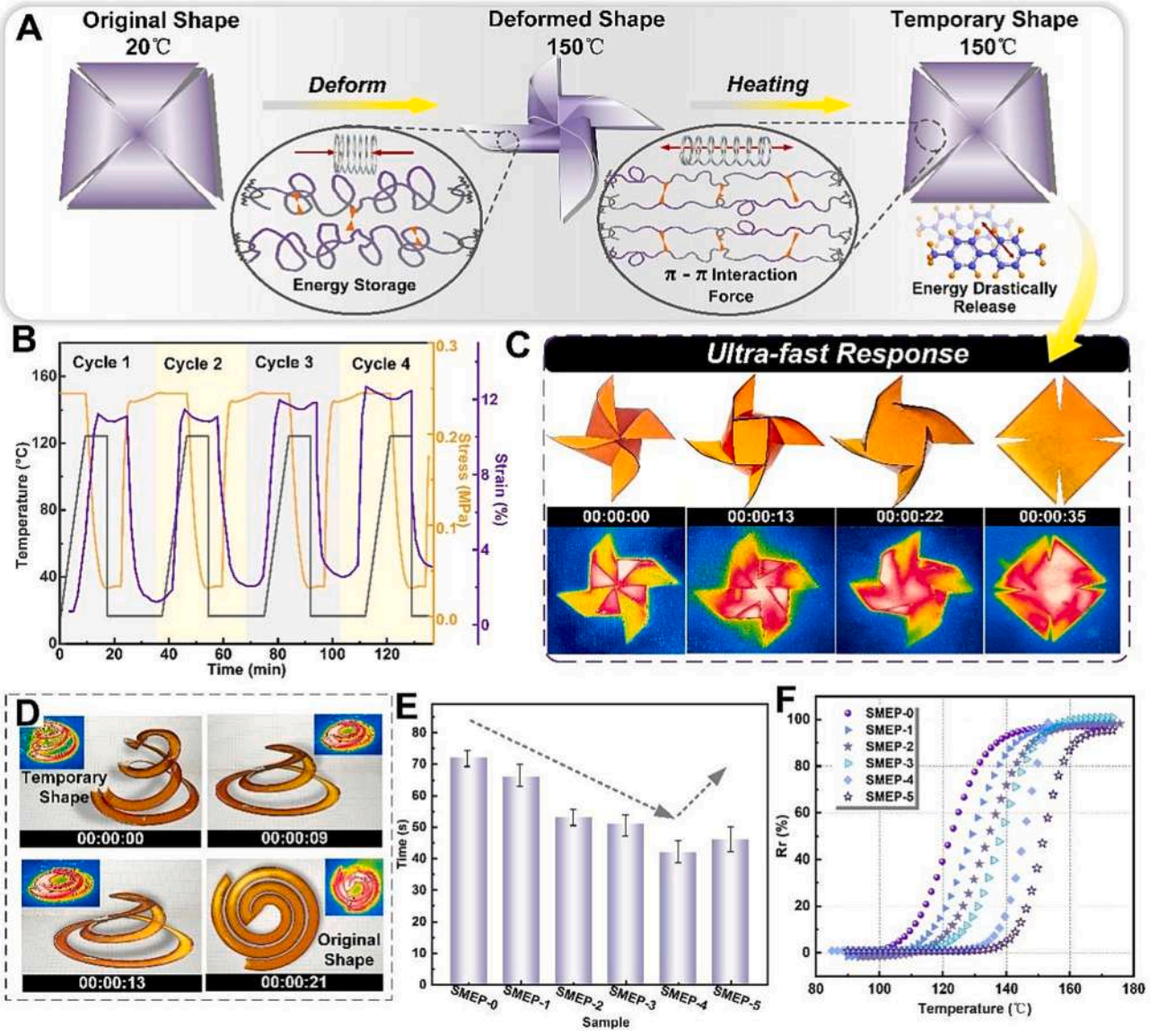

Fig. 7. **(a)** Schematic diagram of shape memory molecules of SMEPs. **(b)** Shape memory cycle test curve for the SMEP-4. **(c, d)** Shape recovery process for SMEP-4 samples. **(e)** The shape recovery time of the SMEPs. **(f)** The samples from the SMEPs follow these shape reversion process curves.

3.4. Shape memory behavior

The rigidity and stability of the resin can be increased by adding a benzene ring. Additionally, it strengthens the intermolecular contact forces and further enhances shape memory performance by increasing the π-π stacking interaction between molecules. The performance of thermosetting shape memory resins can be improved via hydrogen bonding. Additionally, the greater the number of hydrogen bonds, the stronger the intermolecular interaction forces. Hydrogen bonding between molecules can enhance the intermolecular interaction forces and improve shape memory performance (Fig. 7**a**). The regularly arranged structure of benzene rings and hydrogen bonds can give polymers a certain degree of elasticity and plasticity. Elasticity allows the material to deform elastically when a force is applied and to return to its original state when the stress is removed. The results of the shape memory performance of a four-cycle test of the SMEP-4 sample using DMA are shown in Fig. 7**b.** Both the shape recovery and fixity rates were determined to be greater than 95 %. The spiral and windmill structures at Tg gradually unfold, as shown in Fig. 7**c and d.** The SMEP-4 for wind models can quickly return to its original shape in 35 s. This is owing to SMPs with a high benzene ring concentration having a high modulus of elasticity and robustness, which may quickly recover to their previous state after deformation. Second, as an organized molecular arrangement structure, the benzene ring enhances molecule interaction and mobility while also promoting shape memory recovery. Demonstrating the excellent shape-memory performance of the SMEP. The sample was made into a spiral structure and the surface temperature was recorded under a 150° heat source. Complete shape recovery within 21 s. The inherent thermal conductivity of SMEP accelerates recovery (Movie S3 and Movie S4). The shape recovery times of the SMEP system at each Tg are shown in Fig. 7**e**. It is worth noting that the shape recovery time comparison between SMEP-3 and SMEP-5 is longer for SMEP-3 than for SMEP-5. For this we carried out a detailed comparison to find out. After comparing the properties of tensile strength, thermal conductivity, it was found that SMEP-3 and SMEP-5 have nearly similar properties. However, the modulus of SMEP-5 is also higher than that of SMEP-3, as shown in Fig. 4**f.** When the content of PPDP increases by 20 wt%, the ordered arrangement and high-density spherical structure formed in the polymer can provide additional energy barriers. Under temperature stimulation, the driving force of shape memory recovery is enhanced, and the speed of shape memory recovery is improved. The graph clearly shows that samples with higher thermal conductivities recovered more rapidly. Moreover, samples with higher moduli can produce more power during recovery, which helps overcome external resistance and hasten

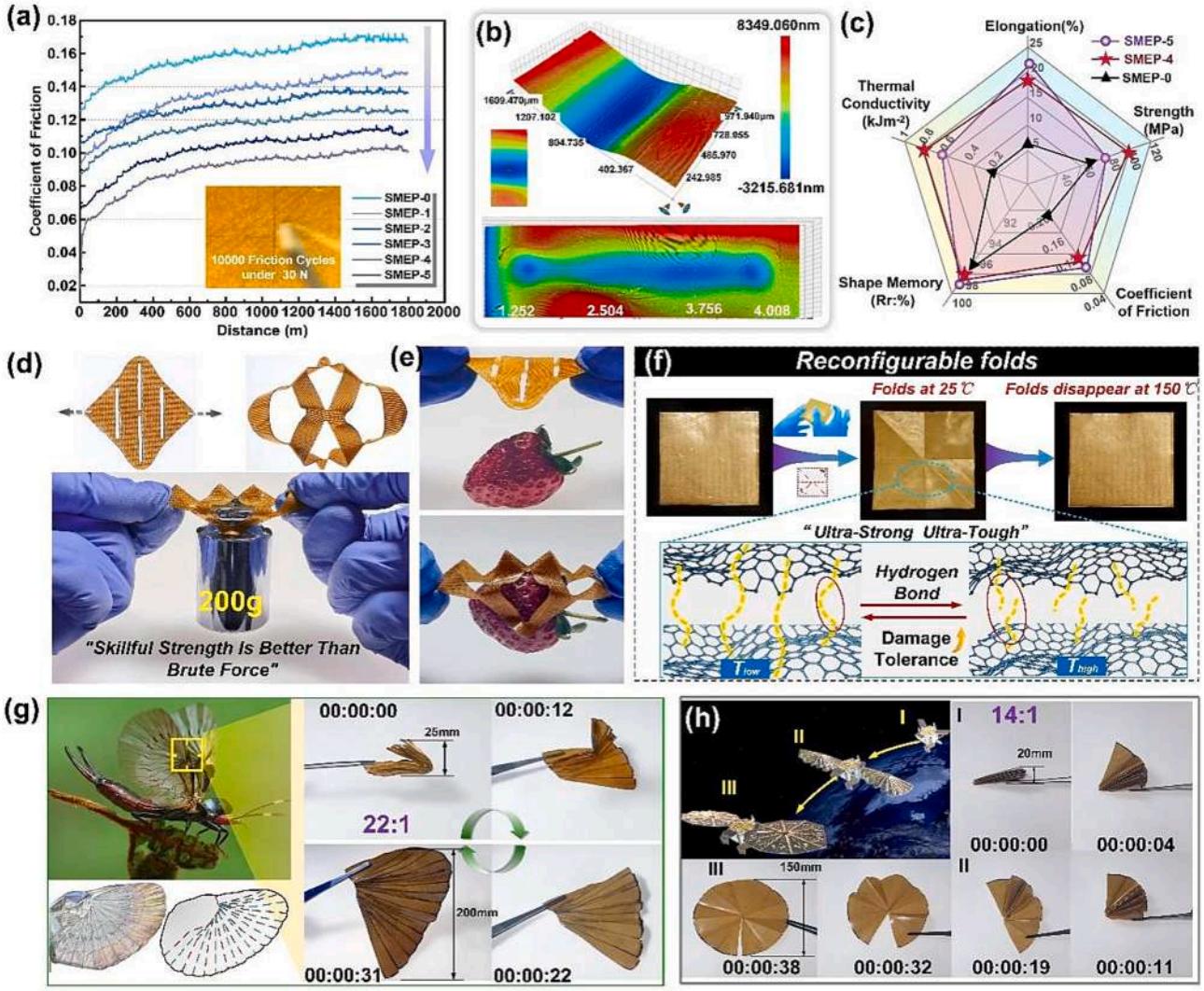

Fig. 8. **(a)** Friction coefficients for SMEPs systems. **(b)** 3D depth-of-field image of SMEP-1 after friction test. **(c)** Performance comparison radar plot for SMEPs. **(d)** SMEP-4 can lift weights weighing up to 200 g. **(e)** The gripper structure of SMEP-4 can grip strawberries. **(f)** Schematic diagram of reconfigurable folds. **(g)** "Earwig" folding wing structure. **(h)** High fold-to-spread ratio structure for solar array.

recovery. The recovery response temperature was consistent with the shift in the Tg (Fig. 7**f**). With the decrease in the PPDP content, the deformation response temperature of the material also shifted to lower temperatures, effectively adjusting the shape response temperature of the shape memory liquid crystal epoxy resin. Notably, SMPs have high thermal conductivity, which enables them to rapidly adjust to changes in the ambient temperature.

3.5. Application potential

The sample was subjected to a wear experiment with 10,000 repetitions under a load of 30 N, and the friction coefficient was determined (Fig. 8**a**). It maintained its mechanical performance through 10,000 friction cycles, demonstrating a high reliability. The SMEP system exhibits a low friction coefficient due to the potential impact of the polymer's molecular structure on frictional performance. A decreased friction coefficient is produced by the weak intermolecular contact forces of the straight-chain polycyclic aromatic polymer. Moreover, the molecular organized, and the intermolecular contact forces increase with the increase in the degree of crystallization, which increases the friction coefficient. The 3D morphology image of the sample after reciprocal friction is depicted in Fig. 8**b**. The crystalline structure has an orderly molecular arrangement, making the surface of the material smoother and stronger. This structure effectively resists friction and abrasion, increasing the material's wear resistance. The overview of SMEP is shown in Fig. 8**c,** which is due to the multidimensional network structure of the π-π bond and hydrogen bond-connected segments of the liquid crystal main chain that we designed and constructed. It has demonstrated excellent performance of thermosetting epoxy resins, including high strength, high toughness, extreme cold temperature resistance, friction, and intrinsic thermal conductivity. The SMEPs can be used as a structural material for origami because of their strength and toughness. More significantly, the folds vanish at high temperatures, allowing for a reconfigurable shape. We decided on a straightforward paper-cut thin shell to achieve precision robotic grasping[45] (see Movie S5). The distinction is that we do not need to merge the paper sheet with the cut seam; instead, we can achieve active self-folding and picking behavior by utilizing the variable stiffness property, which can sustain high stiffness at room temperature and lift 200 g, 20 times its weight (Fig. 8**d**). Owing to its low rigidity, it can be used as a soft grip to pick up delicate objects, such as strawberries, at high temperatures (Fig. 8**e,** see Movie S6). Fig. 8**f** is a schematic diagram of reconfigurable folding. We folded the sample at room temperature, leaving creases. This is due to the high strength and toughness of the sample, which greatly increases the damage limit of the material. The presence of hydrogen bonds causes fracture rearrangement at high temperatures, and the creases gradually disappear. Due to the variable stiffness characteristics of the material, the creases disappear at Tg and have the characteristic of repeated folding, meaning that a thin film can be refoldable without leaving any creases. This feature is not possible with general shape memory thermoset resins. Additionally, in line with the origami structure, we replicated the combinatorial folding of the earwig, as shown in Fig. 8**g**, mimicking the natural folding system of an earwig wing with a stowage ratio of 22:1. The variable stiffness offers a self-locking feature and works in conjunction with the bending stiffness for simple flutter flight. SMEPs in large solar panels on satellites that unfold in orbit to produce a regulated unfolding function with a high fold-to-spread ratio (18:1) allow for the most efficient use of limited space (Fig. 8**h,** see Movie S7).

4. Conclusion

In this study, a reconfigurable shape memory epoxy resin multidimensional cross-linked network structure is reported. The π-π and hydrogen bonds synergistically expand the thermal conductivity transmission pathway, resulting in a cross-linked network with enhanced thermal conductivity. The polymerization strategy of covalent and noncovalent bonds breaks the contradiction between strength and toughness. It can lift 10,000 times its weight, and the ultimate bending curvature can reach 0.99 mm. With the function of refoldability, this mechanism increases the material's ability to withstand damage and causes the crease it produces at room temperature to vanish at high temperatures. Remarkably, these novel polymers display a high degree of flexibility in extremely cold settings (-190 °C) and excellent wear resistance that maintains their mechanical properties under 10,000 friction cycles, showing a high level of dependability. This study has enabled the development of a new generation of materials with high toughness and strength. The intrinsic thermal conductivity SMEP, which can fold and reconfigurable high temperature creases at room temperature, has good application prospects. High folding ratio deployment structures in aerospace, as well as rigid and flexible robots grasping materials.

CRediT authorship contribution statement

Lan Luo: Conceptualization, Methodology, Investigation, Writing – review & editing. **Fenghua Zhang:** Conceptualization, Methodology, Investigation, Validation. **Linlin Wang:** Methodology, Validation. **Yanju Liu:** Conceptualization, Supervision, Writing – review & editing. **Jinsong Leng:** Conceptualization, Funding acquisition, Supervision.

Declaration of competing interest

The authors declare that they have no known competing financial interests or personal relationships that could have appeared to influence the work reported in this paper.

Data availability

Data will be made available on request.

Acknowledgments

We thank National Key R&D Program of China (2022YFB3805700) and National Natural Science Foundation of China (Grant No. 92271112) for the support of this work.

Appendix A. Supplementary data

Supplementary data to this article can be found online at https://doi.org/10.1016/j.cej.2023.147428.

References

[1] J. Leng, X. Lan, Y. Liu, S. Du, Shape-memory polymers and their composites: Stimulus methods and applications, Prog. Mater Sci. 56 (7) (2011) 1077–1135, https://doi.org/10.1016/j.pmatsci.2011.03.001.
[2] J. Wang, L. Sun, M. Zou, W. Gao, C. Liu, L. Shang, Z. Gu, Y. Zhao, Bioinspired shape-memory graphene film with tunable wettability, Science, Advances 3 (6) (2017), https://doi.org/10.1126/sciadv.1700004.
[3] L. Luo, F. Zhang, J. Leng, Shape Memory Epoxy Resin and Its Composites: From Materials to Applications, Research 2022 (2022), https://doi.org/10.34133/2022/9767830.
[4] X. Wang, Y. He, Y. Liu, J. Leng, Advances in shape memory polymers: Remote actuation, multi-stimuli control, 4D printing and prospective applications, Materials Science & Engineering R-Reports 151 (2022), https://doi.org/10.1016/j.mser.2022.100702.
[5] L. Luo, F. Zhang, Y. Liu, J. Leng, Super-tough, self-sensing and shape-programmable polymers via topological structure crosslinking networks, Chem. Eng. J. 457 (2023), https://doi.org/10.1016/j.cej.2023.141282.
[6] M.A. Kouka, F. Abbassi, M. Habibi, F. Chabert, A. Zghal, C. Garnier, 4D Printing of Shape Memory Polymers, Blends, and Composites and Their Advanced Applications: A Comprehensive Literature Review, Adv. Eng. Mater. 25 (4) (2023), https://doi.org/10.1002/adem.202200650.
[7] X. Pang, J.-A. Lv, C. Zhu, L. Qi, Y. Yu, Photodeformable Azobenzene-Containing Liquid Crystal Polymers and Soft Actuators, Adv. Mater. 31 (52) (2019), https://doi.org/10.1002/adma.201904224.

[8] Y. Liu, W. Wu, J. Wei, Y. Yu, Visible Light Responsive Liquid Crystal Polymers Containing Reactive Moieties with Good Processability, ACS Appl. Mater. Interfaces 9 (1) (2017) 782–789, https://doi.org/10.1021/acsami.6b11550.
[9] W.M. Huang, Z. Ding, C.C. Wang, J. Wei, Y. Zhao, H. Purnawali, Shape memory materials, Mater. Today 13 (7–8) (2010) 54–61, https://doi.org/10.1016/s1369-7021(10)70128-0.
[10] C. Liu, S. Ji, H. Xu, Rapidly reprogrammable actuation of liquid crystal elastomers, Matter 5 (8) (2022) 2409–2413, https://doi.org/10.1016/j.matt.2022.05.009.
[11] J.A.C. Liu, J.H. Gillen, S.R. Mishra, B.A. Evans, J.B. Tracy, Photothermally and magnetically controlled reconfiguration of polymer composites for soft robotics, Science, Advances 5 (8) (2019), https://doi.org/10.1126/sciadv.aaw2897.
[12] Z. Liu, Q. Li, W. Bian, X. Lan, Y. Liu, J. Leng, Preliminary test and analysis of an ultralight lenticular tube based on shape memory polymer composites, Compos. Struct. 223 (2019), https://doi.org/10.1016/j.compstruct.2019.110936.
[13] L. Luo, F. Zhang, W. Pan, Y. Yao, Y. Liu, J. Leng, Shape memory polymer foam: active deformation, simulation and validation of space environment, Smart Mater. Struct. 31 (3) (2022), https://doi.org/10.1088/1361-665X/ac4ba8.
[14] X. Lan, L. Liu, C. Pan, F. Li, Z. Liu, G. Hou, J. Sun, W. Dai, L. Wang, H. Yue, Y. Liu, J. Leng, X. Zhong, Y. Tang, Smart Solar Array Consisting of Shape-Memory Releasing Mechanisms and Deployable Hinges, AIAA J. 59 (6) (2021) 2200–2213, https://doi.org/10.2514/1.J059281.
[15] J. Sun, B. Peng, Y. Lu, X. Zhang, J. Wei, C. Zhu, Y. Yu, A Photoorganizable Triple Shape Memory Polymer for Deployable Devices, Small 18 (9) (2022), https://doi.org/10.1002/smll.202106443.
[16] F. Zhang, N. Wen, L. Wang, Y. Bai, J. Leng, Design of 4D printed shape-changing tracheal stent and remote controlling actuation, International Journal of Smart and Nano Materials 12 (4) (2021) 375–389, https://doi.org/10.1080/19475411.2021.1974972.
[17] S. Liu, Q.-S. Yang, Finite element analysis of shape-memory polymer mast, International Journal of Smart and Nano Materials 10 (4) (2019) 285–299, https://doi.org/10.1080/19475411.2019.1686666.
[18] C. Sealy, Shape memory polymer responds to biological activity, Mater. Today 25 (2019) 6, https://doi.org/10.1016/j.mattod.2019.03.004.
[19] S. Miao, N. Castro, M. Nowicki, L. Xia, H. Cui, X. Zhou, W. Zhu, S.-J. Lee, K. Sarkar, G. Vozzi, Y. Tabata, J. Fisher, L.G. Zhang, 4D printing of polymeric materials for tissue and organ regeneration, Mater. Today 20 (10) (2017) 577–591, https://doi.org/10.1016/j.mattod.2017.06.005.
[20] Y. Yang, H. Wang, S. Zhang, Y. Wei, X. He, J. Wang, Y. Zhang, Y. Ji, Vitrimer-based soft actuators with multiple responsiveness and self-healing ability triggered by multiple stimuli, Matter 4 (10) (2021) 3354–3365, https://doi.org/10.1016/j.matt.2021.08.009.
[21] Y. Liu, L. Wang, H. Lu, Z. Huang, High-strength shape-memory organohydrogel based on two orthogonal supramolecular effect: Gelator-induced phase-transition and metal-coordination interaction, Chem. Eng. J. 431 (2022), https://doi.org/10.1016/j.cej.2021.133338.
[22] W.M. Huang, B. Yang, Y. Zhao, Z. Ding, Thermo-moisture responsive polyurethane shape-memory polymer and composites: a review, J. Mater. Chem. 20 (17) (2010) 3367–3381, https://doi.org/10.1039/b922943d.
[23] D. Thanh Duc, H. Ngoc San, N.S. Goo, W.-r., Yu, Design, fabrication, and bending test of shape memory polymer composite hinges for space deployable structures, J. Intell. Mater. Syst. Struct. 29 (8) (2018) 1560–1574, https://doi.org/10.1177/1045389x17742728.
[24] Q. Zhao, H.J. Qi, T. Xie, Recent progress in shape memory polymer: New behavior, enabling materials, and mechanistic understanding, Prog. Polym. Sci. 49–50 (2015) 79–120, https://doi.org/10.1016/j.progpolymsci.2015.04.001.
[25] Q. Zhao, W. Zou, Y. Luo, T. Xie, Shape memory polymer network with thermally distinct elasticity and plasticity, Science, Advances 2 (1) (2016), https://doi.org/10.1126/sciadv.1501297.
[26] M. Zare, M.P. Prabhakaran, N. Parvin, S. Ramakrishna, Thermally-induced two-way shape memory polymers: Mechanisms, structures, and applications, Chem. Eng. J. 374 (2019) 706–720, https://doi.org/10.1016/j.cej.2019.05.167.
[27] M.J. Jo, H. Choi, G.H. Kim, W.-R. Yu, M. Park, Y. Kim, J.K. Park, J.H. Youk, Preparation of Epoxy Shape Memory Polymers for Deployable Space Structures Using Flexible Diamines, Fibers Polym. 19 (9) (2018) 1799–1805, https://doi.org/10.1007/s12221-018-8549-5.
[28] X. Xu, J. Zhou, J. Chen, Thermal Transport in Conductive Polymer-Based Materials, Adv. Funct. Mater. 30 (8) (2020), https://doi.org/10.1002/adfm.201904704.
[29] S. Li, X. Yu, H. Bao, N. Yang, High Thermal Conductivity of Bulk Epoxy Resin by Bottom-Up Parallel-Linking and Strain: A Molecular Dynamics Study, J. Phys. Chem. C 122 (24) (2018) 13140–13147, https://doi.org/10.1021/acs.jpcc.8b02001.
[30] Y. Lin, X. Huang, J. Chen, P. Jiang, Epoxy thermoset resins with high pristine thermal conductivity, High Voltage 2 (3) (2017) 139–146, https://doi.org/10.1049/hve.2017.0120.
[31] Y. Xu, X. Wang, J. Zhou, B. Song, Z. Jiang, E.M.Y. Lee, S. Huberman, K.K. Gleason, G. Chen, Molecular engineered conjugated polymer with high thermal conductivity, Science, Advances 4 (3) (2018), https://doi.org/10.1126/sciadv.aar3031.
[32] X. Zhong, X. Yang, K. Ruan, J. Zhang, H. Zhang, J. Gu, Discotic Liquid Crystal Epoxy Resins Integrating Intrinsic High Thermal Conductivity and Intrinsic Flame Retardancy, Macromol. Rapid Commun. 43 (1) (2022), https://doi.org/10.1002/marc.202100580.
[33] X. Shen, Y. Gao, Y. Sun, D. Bao, F. Xu, Y. Cui, H. Wang, Y. Zhu, H. Huang, Improving the Intrinsic Thermal Conductivity of Epoxy Resin by Synergistic Effect between Rigid Groups and Hydrogen Bonds, ChemistrySelect 6 (32) (2021) 8219–8226, https://doi.org/10.1002/slct.202102175.
[34] Y. Li, C. Liu, W. Zhou, Z. Hou, Q. Shi, C. Gong, Y. Wu, Microscopic ordered structure compactness and intrinsic thermal conductivity improvement of dispersed liquid crystal films of flexible epoxy-thiol polymers, Mater. Today Commun. 29 (2021), https://doi.org/10.1016/j.mtcomm.2021.102792.
[35] Y. Li, C. Gong, Z. Hou, W. Zhou, C. Liu, L. Peng, Y. Wu, Q. Shi, Q. Cheng, Flexible epoxy-dispersed liquid crystal membranes of intrinsic thermal conductivity with high voltage orientation molding, J. Appl. Polym. Sci. 139 (44) (2022), https://doi.org/10.1002/app.53077.
[36] S.J. Yuan, Z.Q. Peng, M.Z. Rong, M.Q. Zhang, Enhancement of intrinsic thermal conductivity of liquid crystalline epoxy through the strategy of interlocked polymer networks, Mater. Chem. Front. 6 (9) (2022) 1137–1149, https://doi.org/10.1039/d2qm00090c.
[37] J. Dang, J. Zhang, M. Li, L. Dang, J. Gu, Enhancing intrinsic thermal conductivities of epoxy resins by introducing biphenyl mesogen-containing liquid crystalline co-curing agents, Polym. Chem. 13 (42) (2022) 6046–6053, https://doi.org/10.1039/d2py01157c.
[38] T. Xie, I.A. Rousseau, Facile tailoring of thermal transition temperatures of epoxy shape memory polymers, Polymer 50 (8) (2009) 1852–1856, https://doi.org/10.1016/j.polymer.2009.02.035.
[39] N. Zheng, G. Fang, Z. Cao, Q. Zhao, T. Xie, High strain epoxy shape memory polymer, Polym. Chem. 6 (16) (2015) 3046–3053, https://doi.org/10.1039/c5py00172b.
[40] F. Xie, L. Huang, J. Leng, Y. Liu, Thermoset shape memory polymers and their composites, J. Intell. Mater. Syst. Struct. 27 (18) (2016) 2433–2455, https://doi.org/10.1177/1045389x16634211.
[41] G.P. Tandon, K. Goecke, K. Cable, J. Baur, Durability Assessment of Styrene- and Epoxy-based Shape-memory Polymer Resins, J. Intell. Mater. Syst. Struct. 20 (17) (2009) 2127–2143, https://doi.org/10.1177/1045389x09348255.
[42] Y. Zhao, D. Zhang, L. Guo, Shape-memory behavior of bisphenol A-type cyanate ester/carboxyl-terminated liquid nitrile rubber coreacted system, Colloid Polym. Sci. 292 (10) (2014) 2707–2713, https://doi.org/10.1007/s00396-014-3321-x.
[43] Q. Zhang, H. Wei, Y. Liu, J. Leng, S. Du, Triple-shape memory effects of bismaleimide based thermosetting polymer networks prepared via heterogeneous crosslinking structures, RSC Adv. 6 (13) (2016) 10233–10241, https://doi.org/10.1039/c5ra24247a.
[44] H. Schaefer, A. Hartwig, K. Koschek, The nature of bonding matters: Benzoxazine based shape memory polymers, Polymer 135 (2018) 285–294, https://doi.org/10.1016/j.polymer.2017.12.029.
[45] Y. Yang, K. Vella, D.P. Holmes, Grasping with kirigami shells, Science, Robotics 6 (54) (2021), https://doi.org/10.1126/scirobotics.abd6426.